

## Photothermal Conversion Characteristics of Silver Nanoparticle Dispersions

Dongsheng WEN<sup>1\*</sup>, Hui ZHANG<sup>2</sup>, Hui-Jiuan CHEN<sup>1</sup>, Guiping LIN<sup>3</sup>

\* Corresponding author: Tel.: ++44 (0)113 3431299; Fax: ++44 (0)113 3431009; Email: d.wen@leeds.ac.uk

1 School of Chemical and Process Engineering, University of Leeds, UK

2 School of School of Energy and Power, North China Electric Power University, China

3 School of Aeronautic Science and Engineering, Beijing University of Aeronautics and Astronautics, China

**Abstract** Nanoparticle-based direct absorption system is a recent development, which employs nanoparticles to absorb and convert solar energy directly into thermal energy within the fluid volume. This work reports for the first time the use of plasmonic nanoparticles (PNPs) to improve the direct photo-thermal conversion efficiency. Rod-shaped silver nanoparticles are synthesized and used as an example to illustrate the photo-thermal conversion characteristics of PNPs and the effect of particle shape. The result reveals a significant role of particle morphology on the photo-thermal conversion efficiency (PTE). For spherical silver particles, constant specific absorption rate (SAR), ~0.14 kW/g, is observed and the PTE increases nearly linearly with the particle concentration. For rod-shaped silver nanoparticles, much higher SARs (2~5 kW/g) are obtained, and the PTE increases from 43% (pure DI water) to 61% at a low concentration of 0.0028%. It is suggested that the increased specific surface area and the absorption spectrum variation are the two main reasons for the strong heating effect of rod-shaped silver nanoparticles.

**Keywords:** Plasmonic nanoparticle, silver, nanofluids, nanowire, photo-thermal conversion, solar collector

### 1. Introduction

The heat transfer properties of nanofluids, i.e., suspensions of nanoparticles in liquids, have been extensively studied in the last two decades. The effective properties of the nanofluid system such as thermal conductivity, viscosity and surface tensions can be significantly modified by the inclusion of different nanoparticles [Buongiorno et al 2009, Venerus et al. 2010]. Nanoparticle-based direct absorption (NDA) system is a recent development, which employs nanoparticles to absorb and convert solar energy directly into thermal energy within the fluid volume [Otanicar et al. 2009]. Such a process would overcome the limitations of conventional surface-controlled solar thermal systems. Comparing to the conventional idea of direct absorptions that originated in 1970's [Arai et al.], the reduction of particle size to the nanometer scale offers additional benefits such as increased surface-to-volume ratios and size-dependent radiation properties. Properly designed, NDA could simplify the conventional solar thermal system and improve the photo-thermal conversion

efficiencies.

The radiation properties of a few nanomaterials were experimentally investigated [Sani et al. 2010, Otanicar et al. 2010, Taylor et al. 2011, Sani et al. 2011, Han et al. 2011, Lenert and Wang 2012, He et al. 2013] and theories were proposed to maximize the photo-thermal conversion efficiency under optimized particle concentrations [Tyagi et al. 2007, Otanicar et al. 2009 and Otanicar et al. 2010, Taylor et al 2011, Fang et al. 2013]. For instance, Otanicar et al. (2010) showed that the overall thermal efficiency of the collector could be improved by 5% by utilizing different nanoparticle dispersions (i.e., carbon nanotube, graphite and silver). Sani et al. (2011) and Mercatelli et al. (2011) investigated the absorption properties of single-wall based carbon nanohorn-based nanofluids for direct sunlight absorbers with water and ethylene glycol as base fluids. The carbon nanohorn consists of a single layer of a graphene sheet wrapped into an irregular tube with a variable diameter of generally 2-5 nm, a length of 30-50 nm, and a cone-shaped angle of 20 degree. Comparing with the base

fluid, and also carbon black nanofluids, the measured absorption coefficient showed a remarkable improvement over a wide spectral range, which suggests that particle shape plays a significant role in the direct solar energy absorption. Lenert and Wang (2012)'s study showed that the receiver efficiency increased with increasing nanofluid height and incident solar flux, and there existed an optimum optical thickness. He et al. (2013) reported that the maximum bulk temperature rise of an aqueous medium seeded by 0.1 w% copper nanoparticles (~50 nm) can be increased to 25%. However the lack of proper control in nanomaterials (i.e., size, shape and concentration) makes it is difficult to study the particle morphology effect and also difficult to compare among different research groups.

The investigation of plasmonic particles for direct solar-thermal energy conversion is seldom reported, although it is known in the physics that significant heat can be induced through the surface plasmon resonance process (SPR) [Hu 2006, Panyala 2009, Becker 2010, Liu et al. 2012]. This work aims to investigate the photo-thermal conversion efficiency of one particular plasmonic particle, silver nanoparticle, with a particular focus on the effect of particle shape.

## 2 Experimental approach

### 2.1 Silver nanoparticle synthesis and characterization

There are many methods of producing silver nanoparticles with different shapes. In this work, silver nanorods were synthesized through reducing  $\text{AgNO}_3$  with ethylene glycol (EG) in the presence of poly(vinyl pyrrolidone) (PVP) (Zhu et al., 2007). Briefly, 6 ml of EG solvent was heated to  $150^\circ\text{C}$ , and then 2 ml of 0.2 mol of  $\text{AgNO}_3$  dissolved in EG was added. Following that, 2 ml of EG containing 0.1 gram of PVP (molecular weight = 10,000) was added dropwise within a period of 3 minutes. The solution was stirred and heated for further 45 minutes. Finally 20 ml acetone was added and the resultant suspension was centrifuged to

remove EG and PVP. The solid particles were dried and re-dispersed in DI water, stored under the room temperature.

The resulting silver nanoparticles are rod-shaped, as shown in Figure 1. They have varied length in the range of 1~5 micrometers, centred about  $2\mu\text{m}$ , and have the length-to-diameter ratio of 10~30. The absorption spectrum of silver nanorod was measured by an UV/Vis spectrometer (PerkinElmer, lambda 35), shown in Figure 2. The absorption wavelength of Ag wires is broad, covering a wide spectral range from 300 nm to 800 nm, and peaking at 420 nm.

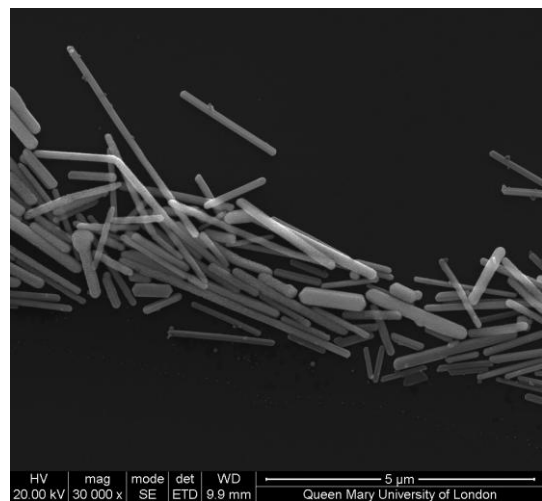


Figure 1. SEM image of synthesized silver nanowire

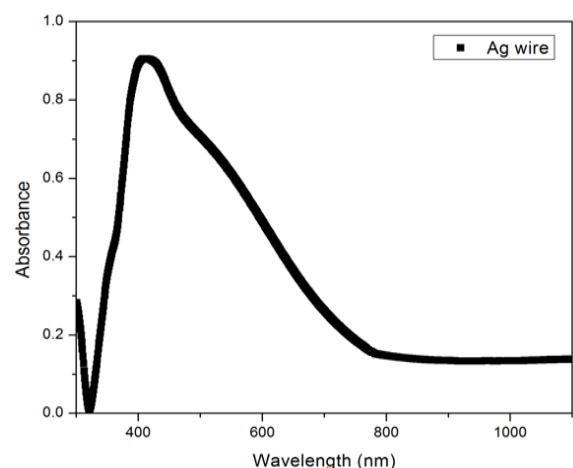


Figure 2: Absorption spectrum of silver wire (concentration = 0.0023%)

## 2.2 Photo-thermal conversion experiment

The photo-thermal conversion experimental setup is shown in Figure 3.

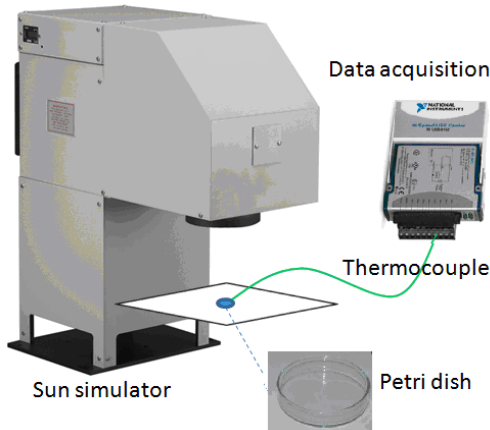


Figure 3 Schematic illustration of the experimental system

In order to minimize the experimental uncertainties under direct sun light, a solar simulator (Newport Co. Oriel Xenon Arc lamp) was used as the light source. It provides a close spectral match to the solar spectra, and can vary the radiation intensity between AM1.0 and AM2.0. The performance parameters of the solar simulator are based on the ASTM, including spectral match (fraction of ideal percentage) of 0.7~1.25, non-uniformity of irradiance of up to 5% and temporal instability of up to 5%. To minimize the temperature gradient inside the fluid, a thin layer of silver nanoparticle dispersion (~3mm) was put in a Petri dish (35mm diameter), which was located in the centre spot of the solar simulator. A uniform radiation from the simulator can be assumed. The top of the Petri dish was covered by a glass plate to reduce the radiation from the sample. The centre sample temperature was measured by a K-type thermocouple (Omega 5TC-TT-K-36-36), whose head was fixed on the bottom centre of the Petri dish. The data was recorded in a PC through a data acquisition hardware (thermocouple input devices, NI, USB-9211, 4-Channel, 24-bit) under the Labview environment. Preliminary tests showed that the space variation of the sample temperature is small. The uncertainty of the temperature was estimated as  $\pm 0.25^\circ\text{C}$ . Sample fluid was injected slowly through a

cylindrical injector into the Petri dish before each experiment.

## 3. Results and discussion

An air mass of 1.5, ( $AM = 1.5$ ), which represents the solar spectrum at mid-latitudes, is used in the photo-thermal conversion experiments. At  $AM=1.5$ , the solar intensity ( $I$ ) is  $0.1\text{W}/\text{cm}^2$  according to the standard of ASTM G-173. The sample fluids were heated under the fixed solar intensity for duration of 300 seconds. The transient temperature curves were shown in Figure 4, which clearly shows that low concentrations of silver nanorod can significantly increase the bulk temperature. For example, the bulk temperature increased by  $\sim 10.6\text{ K}$  at a concentration of 0.0028% at the end of 300 seconds, whereas the temperature increase is  $\sim 8.3\text{ K}$  for the pure water. The bulk temperature increases with the increase of particle concentrations, but exhibiting a non-linear feature. At the initial heating stage, the temperature increases nearly linearly with the radiation time, but deviates from the linear feature at the late stage due to the heat dissipation to the surroundings.

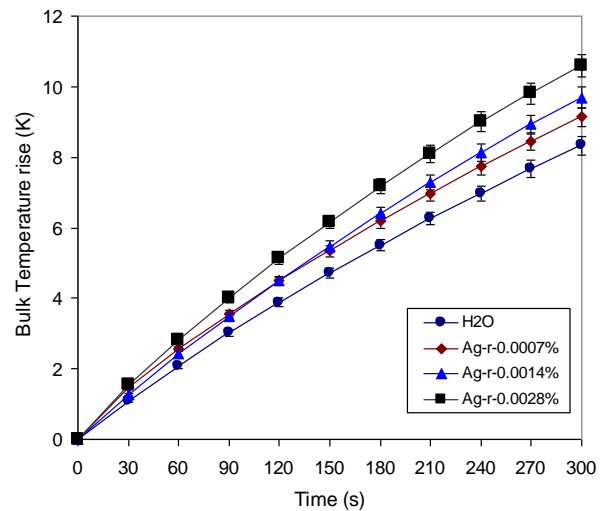


Figure 4: Transient temperature rise of rod-shaped silver nanoparticle dispersions

To compare with the particle shape effect, the photo-thermal conversion of spherical silver nanoparticles were conducted. The dried silver particle was purchased commercially, which has a primary diameter

of  $\sim 10$  nm but in the form of large agglomerates. To perform the experiments, the particles were dispersed into DI water under the help of an ultrasound probe. Figure 5 shows a similar scenario on the bulk temperature as the rod-shaped particle; however the effect of spherical nanoparticle is small under low concentrations. Small bulk temperature increase was observed for particle concentrations of 0.0028 and 0.01%. Significant bulk temperature increase, up to 11.4 K, was shown at a particle concentration of 0.05%. This comparison shows significantly the effect of particle shape on the photo-thermal conversion.

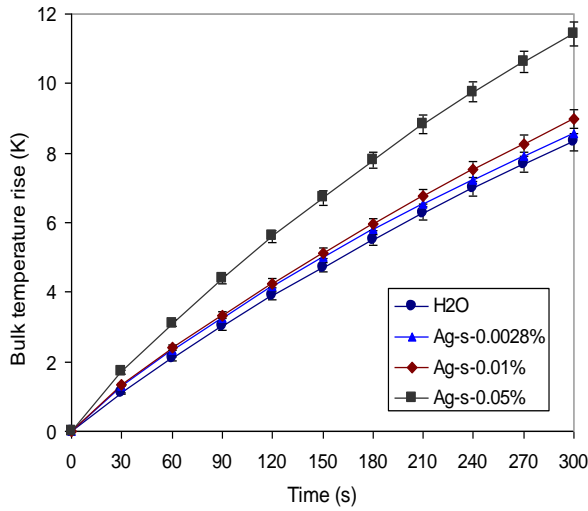


Figure 5: Transient bulk temperature rise of spherical-shaped Ag nanoparticle dispersions

Under low continuous radiation conditions (as in this work), the temperature difference between the particle and the fluid is very small. The temperature of the silver nanoparticle can be assumed to be the same as the surrounding fluid, measured by the thermocouple. As a simple estimation, it can be assumed that the fluid have the same temperature in space under the current experimental setup (i.e., uniform solar radiation and small fluid depth). The photo-thermal conversion efficiency (PTE) ( $\eta$ ) can then be calculated by:

$$\eta = \frac{(c_w m_w + c_p m_p) \Delta T}{IA \Delta t} \quad (1)$$

in which  $c_w$  and  $c_p$  are the specific heat of water and silver particle respectively;  $m_w$  and

$m_p$  are the mass of water and particle respectively;  $\Delta T$  is the temperature rise in a  $\Delta t$  time interval,  $A$  is the illumination area of fluid and  $I$  is the irradiation flux in the experiment. As the particle concentration is so small, i.e.,  $\frac{m_p c_p}{m_w c_w} \sim 0$ , the photo-thermal conversion efficiency can be simplified as:

$$\eta = \frac{c_w m_w \Delta T}{IA \Delta t} \quad (2)$$

The efficiency is proportional directly to the temperature rise gradient. Using the initial temperature rise gradient as an example (i.e. the first 60 second when the heat leak is negligible), the photo-thermal conversion efficiency is calculated, shown in Figure 6. Remarkable performance of silver nanorod is observed even under very small particle concentrations. While for the base fluid alone, the PTE is 44.3%, the efficiency of silver nanorod at a concentration of 0.0028% reaches 61.4%. The enhancement in the PTE of silver nanorod is much higher than other reported materials such as graphite particles ( $\sim 30$  nm diameter) and carbon nanotubes (6–20 nm diameter, 1000–5000 nm in length) (Otanicar 2010) under similar particle concentrations. However for spherical silver particles, similar level of enhancement is observed only at much higher concentrations (i.e. 0.05%).

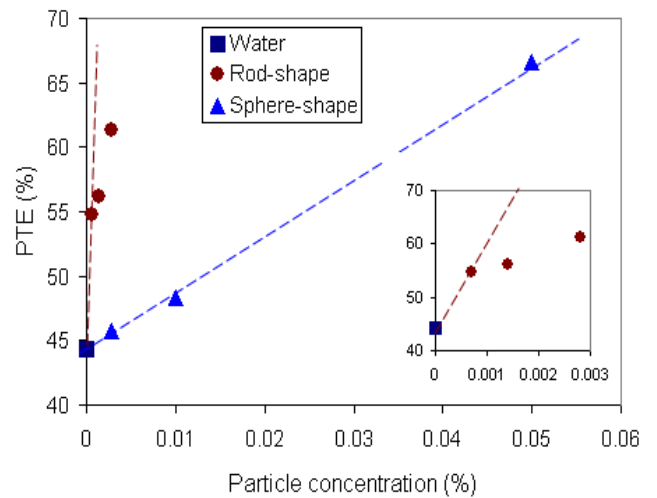


Figure 6: Photothermal conversion efficiency of silver nanoparticles

The reasons for the large difference of

particle shape on the PTE could be ascribed by two factors: i) the surface area effect and ii) the shift in absorption spectrum. As the particle morphology changes from spherical to rod-shape, its surface-to-volume ratios increases and provides more absorption areas. On the other hand, photons can overlap with the plasma resonance of the electrons in the conduction band on the surface of metal nanoparticles to generate collective oscillations, which is commonly known as surface plasmon resonance (SPR). The absorption from the nanoparticle could be greatly enhanced via the coupling of the incident radiation with the collective motion of electrons in metal. By extending the particle morphology to rod-shape, the absorption peak is shifted toward the near-red spectrum, and the absorption spectrum becomes wider, which should also increase the PTE. Both factors shall be responsible for the large effect of rod-shaped silver particles.

It should be noted that very dilute nanoparticle dispersions were used in the experiment (i.e., maximum concentration of 0.05% by weight), and the silver nanoparticles were uniformly dispersed in the base fluid. A simple estimation shows that the  $l/d$  value, i.e., the ratio of the particle-particle distance to the particle diameter, is in the range of 10~100. It is reasonable to consider that the particle-particle interaction should not be important. Silver nanoparticles should act independently in absorbing solar energy according to the scattering regime map [Tien 1988]. Within such a dilute concentration range, it should be reasonable to predict that the enhancement in the photo-thermal conversion efficiency, defined as  $(\eta_n - \eta_w)/\eta_w \cdot 100$  (%), shall increase linearly with the particle concentration. Figure 6 shows that this is true for the spherical silver particles; but it is clearly not the case for the rod-shaped Ag particles, see the insert in Figure 6. Significant enhancement is observed at the lowest particle concentration (0.0007%), and the linearity is broken as the concentration increases. This implied that the photothermal conversion capability per nanoparticle decreases at higher particle loadings.

The decrease in PTE could also be elaborated clearly by a specific absorption rate (SAR) describes the particle's capability in absorbing energy per unit mass, which can be calculated as:

$$SAR = \frac{(m_w c_w + m_p c_p) \Delta T_n - m_w c_w \Delta T_w}{1000 m_p \Delta t} \quad (3)$$

in which  $\Delta T_n$  and  $\Delta T_w$  was the temperature rises at the same  $\Delta t$  time interval for water and nanofluids respectively. Again, as  $\frac{c_p \Delta T_n}{1000 \Delta t} \sim 0$ , the SAR calculation can be simplified as:

$$SAR = \frac{m_w c_w}{1000 m_p} \left( \frac{\Delta T_n}{\Delta t} - \frac{\Delta T_w}{\Delta t} \right) \quad (4)$$

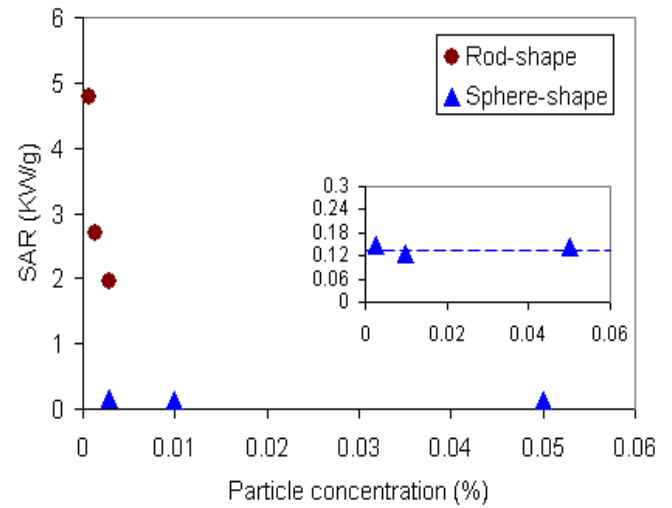


Figure 7: Specific absorption rate of silver nanomaterials

Clearly SAR is proportional to the difference of the temperature rise gradient between the base fluid and the nanofluid. Again using the initial 60s temperature as an example, Figure 7 shows SAR at different particle concentrations. The highest SAR is observed at the lowest concentrations, reaching 4.8 kW per gram for silver nanorod. The SAR value decreases to ~ 2 kW/g when the particle concentration increases from 0.0007% to 0.0028% (i.e., a 4-times increase in concentration). It should be noted that the value of SAR for nanorod silver nanoparticle under such a low heat flux is surprisingly larger than many magnetic nanoparticles under high magnetic fields, which typically in

the order of a few hundred Watt per gram of magnetic nanoparticle [Wen 2009, Wu et al.2010]. This shows the good thermal conversion capability of silver particles. However for spherical silver particles, the SAR keeps a constant value of  $\sim 0.14$  kW/g under the current experimental conditions.

Clearly one interesting question to ask is why the conversion efficiency of individual silver nano-rod decreases with the increase of particle concentration in a region that the particle-particle interaction is negligible. It is expected that three factors should be considered carefully. The first possibility is the likely particle agglomeration. Though the particle concentration increases, the number of particles may not increase proportionally, especially for rod-shaped particles that may be entangled together. The second possibility is related to the effect of the fluid thickness on the volumetric absorption of silver nanoparticles. The absorption efficiency of each particle shall be different at different fluid depth. Finally the heat leak through radiation may become strengthened as the particle concentration exceeding a certain value. Considering the nearly constant SAR of spherical silver nanoparticles under the same experimental setup, it is believed that the particle agglomeration should be main responsible for the decreased SARs of silver nanorod at elevated concentrations.

#### 4. Conclusion

This work investigated experimentally the photo-thermal conversion characteristics of silver nanoparticle dispersions under a controlled solar simulator. Silver nanorods were synthesized and compared with the results of spherical particles, which revealed a significant influence of particle morphology on the photo-thermal conversion. For rod-shaped silver nanoparticles, the PTE increased from 43% (pure DI water) to 61% at a particle concentration of 0.0028%, however the specific absorption rate (SAR) of silver nanorod decreased from 4.8 kW/g to 2 kW/g as the particle concentration increased four-folds, which might be related to the entangled morphology of silver nanorods in the fluid. In

comparison, constant SAR ( $\sim 0.14$  kW/g) was observed for spherical silver particles and the PTE increased nearly linearly with the particle concentration. It is suggested that the increased specific surface area and the absorption spectrum variation should be the main reasons for the strong effect of rod-shaped silver nanoparticles.

#### Acknowledgment

The financial support from the National Science Foundation of China (Grant No. 51228601) is gratefully acknowledged.

#### Reference

- ASTM G-173 ASTM retrieved 1 May 2011.
- Arai N, Itaya Y and Hasatani M. Development of a volume heat-trap type solar collector using a fine-particle semitransparent liquid suspension as a heat vehicle and heat-storage medium. *Solar Energy*, 32, 49-56
- Buongiorno J, Venerus D et al. A benchmark study on the thermal conductivity of nanofluids. *Journal of Applied Physics*, 106(9), 094312, 2009
- Becker J., et al. The Optimal aspect ratio of gold nanorods for plasmonic bio-sensing, *Plasmonics*, 2010(5):161-167.
- Fang, X, Xuan Y and Li Q. Theoretical investigation of the extinction coefficient of magnetic fluid *Journal of Nanoparticle Research* (2013) 15:1652
- He Q, Wang S, Zeng S and Zheng Z. Experimental investigation on photothermal properties of nanofluids for direct absorption solar thermal energy systems. *Energy Conversion and Management*. 73 (2013), 150-157
- Han DX, et al., Thermal properties of carbon black aqueous nanofluids for solar absorption, *Nanoscale Research Letters*, (2011)6:457.
- Hu M., et al. Gold nanostructures: engineering their plasmonic properties for biomedical applications, *Chem. Soc. Rev.*, 2006(35):1084-1094.



- Lenert A. and Wang E. N., Optimization of nanofluid volumetric receivers for solar thermal energy conversion, *Solar Energy*, 86(2012):253-265.
- Liu XL, et al., Low frequency heating of gold nanoparticle dispersions for non-invasive thermal therapies, *Nanoscale*, 2012, 4, 3945.
- Mercatelli L., et al., “Absorption and scattering properties of carbon nanohorn-based nanofluids for direct sunlight absorbers”, *Nanoscale Research Letters* 2011, 6:282.
- Otanicar T. P., Phelan P. E. and Golden J. S., Optical properties of liquids for direct absorption solar thermal energy systems, *Solar Energy*, 83(2009):969-977.
- Otanicar T. P., Phelan P. E., Prasher R. S., Rosengarten G., and Taylor R. A., Nanofluid-based direct absorption solar collector, *J. Renewable Sustainable Energy* 2, 033102 (2010).
- Panyala NR, et al. Gold and nano-gold in medicine: overview, toxicology and perspectives, *Journal of Applied Biomedicine*, 2009(7):75-91.
- Sani E. et al., Carbon nanohorns-based nanofluids as direct sunlight absorbers, *Optics Express*, 2010(18): 5179-5187.
- Sani E. et al., Potential of carbon nanohorn-based suspensions for solar thermal collectors, *Solar Energy Materials & Solar Cells*, 95(2011):2994–3000.
- Taylor R.A., et al., Nanofluid optical property characterization: towards efficient direct absorption solar collectors, *Nanoscale Research Letters* 2011, 6:225.
- Tien C.L., Thermal Radiation in packed and fluidized beds, *Journal of Heat Transfer*, 1988, 110:1230-1242.
- Tyagi, H., Phelan, P. E., and Prasher, R. S., “Predicted Efficiency of a Nano-Fluid Based Direct Absorption Solar Receiver”, *Journal of Solar Energy Engineering*. 2007.
- Venerus D, Buongiorno J, ..... Wen D S.... (2010) Viscosity measurement of colloidal dispersion (nanofluids) for heat transfer applications. *Applied Rheology*, 20 (4), 44582.
- Wen DS, Intracellular hyperthermia: nanobubbles and their biomedical application. *Int J Hyperth* 2009, 25(7):533-541.
- Wu SY., et al. A newly developed Fe-doped calcium sulfide nanoparticles with magnetic property for cancer hyperthermia, *Journal of Nanoparticle Research*, 2010(12):1173-1185.
- Zhu J, Kan C, Xhu X, Wang JG , Han M, Zhao Y, Wang B and Wang G. Synthesis of perfect silver nanocubes by a simple polyol process. *Journal of Materials Research*, 2007, 22, 1479-1485